A new modeling strategy for third-order fast high-performance liquid chromatographic data with fluorescence detection. Quantitation of fluoroquinolones in water samples

Mirta R. Alcaráz, Santiago A. Bortolato, Héctor C. Goicoechea & Alejandro C. Olivieri

Analytical and Bioanalytical Chemistry

ISSN 1618-2642
Volume 407
Number 7

Anal Bioanal Chem (2015)
407:1999-2011
DOI 10.1007/s00216-014-8442-z

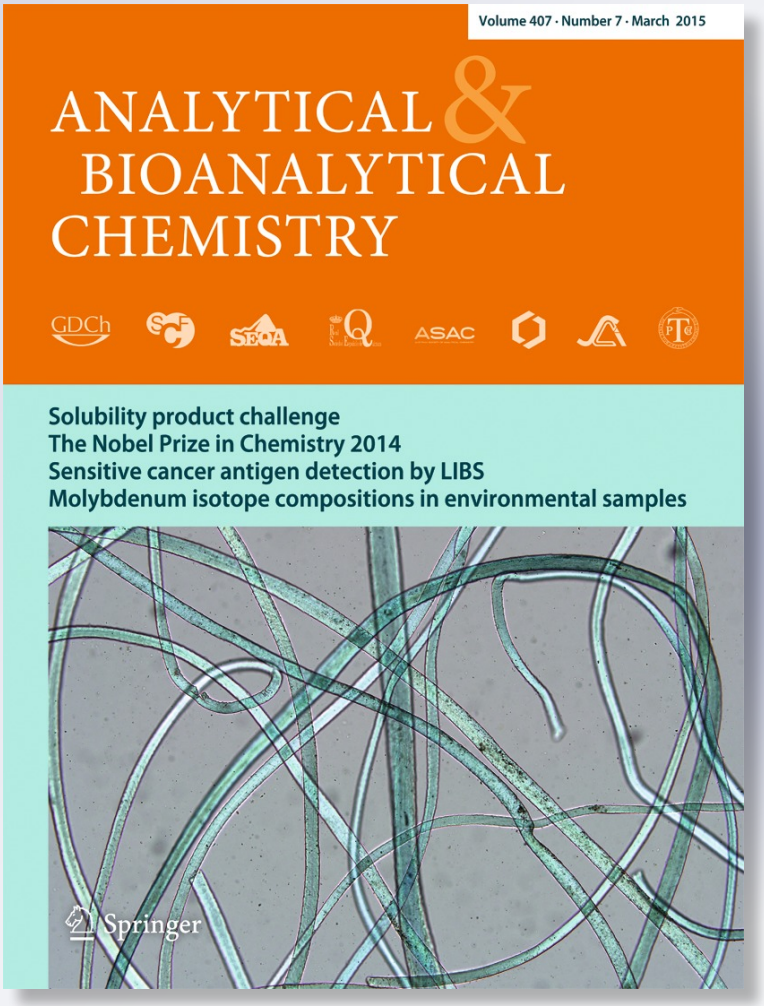

Springer

Anal Bioanal Chem (2015) 407:1999–2011
DOI 10.1007/s00216-014-8442-z

RESEARCH PAPER

A new modeling strategy for third-order fast high-performance liquid chromatographic data with fluorescence detection. Quantitation of fluoroquinolones in water samples

Mirta R. Alcaráz · Santiago A. Bortolato · Héctor C. Goicoechea · Alejandro C. Olivieri

Received: 18 November 2014 / Revised: 17 December 2014 / Accepted: 19 December 2014 / Published online: 21 January 2015

Abstract Matrix augmentation is regularly employed in extended multivariate curve resolution-alternating least-squares (MCR-ALS), as applied to analytical calibration based on second- and third-order data. However, this highly useful concept has almost no correspondence in parallel factor analysis (PARAFAC) of third-order data. In the present work, we propose a strategy to process third-order chromatographic data with matrix fluorescence detection, based on an Augmented PARAFAC model. The latter involves decomposition of a three-way data array augmented along the elution time mode with data for the calibration samples and for each of the test samples. A set of excitation–emission fluorescence matrices, measured at different chromatographic elution times for drinking water samples, containing three fluoroquinolones and uncalibrated interferences, were evaluated using this approach. Augmented PARAFAC exploits the second-order advantage, even in the presence of significant changes in chromatographic profiles from run to run. The obtained relative errors of prediction were ca. 10 % for ofloxacin, ciprofloxacin, and danofloxacin, with a significant enhancement in analytical figures of merit in comparison with previous reports. The results are compared with those furnished by MCR-ALS.

Keywords Liquid chromatography · Third-order data · Fluoroquinolones · Water samples · Augmented parallel factor analysis

Introduction

Nowadays, analytical laboratories have the capacity to generate a wide variety of second- and higher-order instrumental data. Whenever these data are conveniently modeled, significant enhancement in basic analytical properties can be achieved [1]. The implementation of multi-way calibration has become an interesting way to improve the quality of the results when developing analytical methods to be applied for the quantitation of target analytes in complex matrices, such as those present in biological and environmental samples [1, 2].

High performance liquid chromatography (HPLC) can be combined with spectroscopic techniques [UV-visible diode-array detection (DAD), fast-scanning fluorescence detection (FSFD), or mass spectrometric detection (MS)], producing spectral-elution time second-order data [1]. Interestingly, when full selectivity in the chromatographic separation cannot be achieved, second- or higher-order multivariate calibrations can be implemented to the corresponding three- or multi-way arrays, even in the presence of unexpected components, a property known as the second-order advantage [3]. It should be stressed that the application of higher-order calibration in the chromatographic field furnishes additional benefits such as decreasing cost and time of analysis, contributing to the green analytical chemistry principles [4].

Electronic supplementary material The online version of this article (doi:10.1007/s00216-014-8442-z) contains supplementary material, which is available to authorized users.

M. R. Alcaráz · H. C. Goicoechea (✉)
Laboratorio de Desarrollo Analítico y Quimiometría (LADAQ), Cátedra de Química Analítica I, Facultad de Bioquímica y Ciencias Biológicas, Universidad Nacional del Litoral-CONICET, Ciudad Universitaria, 3000 Santa Fe, Argentina
e-mail: hgoico@fbcb.unl.edu.ar

S. A. Bortolato · A. C. Olivieri (✉)
Departamento de Química Analítica, Facultad de Ciencias Bioquímicas y Farmacéuticas, Universidad Nacional de Rosario, Instituto de Química de Rosario (IQUIR-CONICET), Suipacha 531, Rosario S2002LRK, Argentina
e-mail: olivieri@iquir-conicet.gov.ar

As regards third-order multivariate calibration, suitable data arrays can be generated with chromatographic systems equipped with a proper detection device. One common example of third-order data involving chromatography is comprehensive two-dimensional gas chromatography coupled to (time of flight) mass spectrometric detection (GC×GC-TOFMS) [5]. Another example is the recording of excitation-emission matrices (EEMs) as a function of elution time. In the latter case, a first attempt was recently made by performing several chromatographic runs, and recording the emission spectra for every run at a different excitation wavelength across the excitation spectra of the compounds of interest. This methodology was applied to the determination of chlorophylls *a* and *b* and pheophytins *a* and *b* in olive oil [6]. Another procedure for third-order data generation was carried out collecting chromatographic fractions every 2 s, obtaining an EEM for each collected fraction. This methodology was applied for quantitative purposes for the first time, allowing the quantitation of two quinolones in water samples in the presence of unknown components [7].

In theory, it is possible to extend the concepts and algorithms associated to second-order data to third-order data [8, 9]. Therefore, several algorithms were proposed to process third-order chromatographic data but, as mentioned above, few practical applications have been reported [6–8]. If the latter data are registered for a group of samples, a four-way array can, in principle, be constructed, in which case the simplest model is the (low-rank) quadrilinear one, implying that: (1) the three instrumental profiles for each constituent are the same in all samples, and (2) the events taking place in the data modes are independent of each other [8]. When this occurs, to extract useful information from the data, four-way parallel factor analysis (PARAFAC) [10] and some variants [11, 12] may be the best choices. In this regard, the data generated in this work (elution time-EEM data) will be quadrilinear if the elution time profiles show no time misalignments among samples. Unfortunately, chromatographic data usually present variations in constituent profiles in the time mode from sample to sample. Multivariate curve resolution coupled to alternating least-squares (MCR-ALS) [13] is one of the most appropriate models for this kind of problem. Under the latter approach, two of the three data modes must be unfolded to create a data matrix for each sample so that the latter could then be arranged into a bilinear super-augmented matrix [5]. The unfolding operation is performed on the modes where the component profiles do not change from sample to sample (i.e., the spectral excitation and emission modes). An alternative is to align or synchronize the data in the elution time mode using warping procedures [14], which may restore the quadrilinearity of the data and make them amenable to PARAFAC modeling. Finally, strategies exist based on PARAFAC variants such as PARAFAC2 [10], which is more flexible regarding changes in elution profiles from sample to sample, although this latter approach is less useful in the presence of interferents [15].

In principle, an Augmented PARAFAC strategy is capable of processing third-order chromatographic-EEM data via a three-way array, which maintains the original data structure [8]. For each test sample, an augmented three-dimensional array in the elution time direction is produced by appending the data for the calibration samples to those for each test sample. The approach is analogous to matrix augmentation in calibration with MCR-ALS, but in the former case, the decomposition of the data in the three modes (exCitation, emission, and augmented elution time) is unique and may not require restrictions.

In sum, if third-order data are quadrilinear, a four-way PARAFAC model would be the best choice, both regarding the retrieval of pure component properties along the different data modes and analyte predictive ability. This would also be the case if non-quadrilinear data of chromatographic origin can be adequately synchronized, although this does not appear to be a straight-forward procedure in the case of complex samples. Better alternatives are those based on augmentation along the elution time mode, such as MCR-ALS and Augmented PARAFAC, to be compared in the present report. Finally, PARAFAC2 appears to be less flexible towards samples containing uncalibrated interferences.

Concerning the target analytes of the present work, fluoroquinolones (FQs) were chosen as models to show the potentiality of the proposed strategy of third-order data generation and pertinent modeling with Augmented PARAFAC. FQs are highly useful antibacterial agents that are widely used in human and veterinary medicine, being administrated in large quantities to humans and animals. Consequently, these drugs end up in wastewaters coming from hospital and municipal emissions, whereas veterinary drugs are excreted by the animals and are released in the manure. Residues of these antibiotics have been reported in the natural environment in many countries [16]. Therefore, monitoring of low quantities of these compounds from different environmental matrices is essential for human health protection and environmental control. A large number of methods for the determination of FQs in environmental waters have been published, especially including liquid chromatography with fluorescence (LC-FD) or mass (LC-MS) detection [17]. Recently, the quantitation of eight quinolones in ground water samples, with ultrasound-assisted ionic liquid dispersive liquid–liquid microextraction, prior to high-performance liquid chromatography and fluorescence detection, has been published, reporting limits of detection between 0.8 and 13 ng L^{-1} [18]. On the other hand, two reports were very recently published proposing methods for quantitation of FQs in water using HPLC-FSFD and capillary electrophoresis with DAD coupled to second-order calibration [19, 20].

In the present report, a study comparing Augmented PARAFAC and MCR-ALS was carried out. The purpose is two-fold: on one hand, we demonstrate that third-order

instrumental data can be processed using a model (Augmented PARAFAC), which best preserves the original data structure, potentially leading to better selectivity and sensitivity. On the other, we show the benefits of the proposed strategy to determine simultaneously three FQs in drinking water samples from different sources, in the presence of uncalibrated compounds. The method is in accordance with the green analytical chemistry principles, since it implies decreasing cost and time of analysis.

Theory

Three-way Augmented PARAFAC

Constituent profiles may change from sample to sample along any of the three instrumental modes of third-order data [8]. However, in our experimental approach, only the elution time mode is affected by these changes. The approach applied at present implies the building of an augmented trilinear (strictly speaking, *low-rank* trilinear) three-way array. Certainly, the augmentation operation should be done along the mode where the profile changes occur among samples. The main advantage of this strategy is that the model could, in principle, be uniquely decomposed into excitation, emission, and augmented elution time profiles without applying any restriction at all [8].

In the present report, the augmented three-way array $\mathbf{X}_{ap}$ is created along a combined sample-elution time mode [8], and has dimensions $P \times K \times L$ ($P=IJ$), where I, J, K, and L are the number of samples, elution times, excitation, and emission wavelengths, respectively. The corresponding Augmented PARAFAC model can be represented by

$$x_{\mathrm{ap},pkl} = \sum_{n=1}^{N} a_{\mathrm{ap},pn} b_{\mathrm{ap},kn} c_{\mathrm{ap,ln}} + e_{\mathrm{ap},pkl} \quad (1)$$

where decomposition is accomplished in three loading matrices $\mathbf{A}_{ap}$, $\mathbf{B}_{ap}$, and $\mathbf{C}_{ap}$, with sizes $P \times N$, $K \times N$, and $L \times N$, respectively (N is the number of responsive components). The model residuals are collected into $\mathbf{E}_{ap}$, whose sum of squared elements is minimized during data processing [21]. The matrix $\mathbf{A}_{ap}$ collects the augmented profiles along the combined sample-elution time modes and carries concentration information regarding the responsive constituents in a similar manner to the profile matrix retrieved in the augmented mode of MCR-ALS ($\mathbf{C}_{mcr}$, see Electronic Supplementary Material).

Augmented PARAFAC can be implemented through a typical alternating least-squares process. The initialization of the model was made from the experimental excitation and emission spectra. The value of N can be estimated by consideration of the Augmented PARAFAC residual error (i.e., the standard deviation of the elements of the array $\mathbf{E}_{ap}$ in Equation 1 [21]. In general, this parameter decreases with increasing N, until it stabilizes at a value compatible with the instrumental noise. A reasonable choice for N is the smallest number of components for which the residual error is not statistically different from the instrumental noise.

After convergence, the matrices $\mathbf{A}_{ap}$, $\mathbf{B}_{ap}$, and $\mathbf{C}_{ap}$ serve to properly characterize the experimental system, since they gather similar information to that furnished by MCR-ALS. Indeed, $\mathbf{B}_{ap}$ contains the excitation spectra, and $\mathbf{C}_{ap}$ the emission spectra of the chemical constituents under investigation. A combined form of these profiles can be found in MCR-ALS into the ($\mathbf{S}_{mcr}^{T}$) matrix of Equation 1S, as shown in the Electronic Supplementary Material. On the other hand, $\mathbf{A}_{ap}$ contains information relative to the analyte concentrations, in the same way as the $\mathbf{C}_{mcr}$ matrix of Equation 1S. In analogy with MCR-ALS, absolute analyte concentrations are obtained after calibration because the three-way array decomposition only provides relative values in $\mathbf{A}_{ap}$. In view of the fact that the resolved chromatographic profile for each component in the matrix $\mathbf{A}_{ap}$ consists of merged calibration and test profiles, caution must be taken when building the univariate calibration graph against analyte concentrations. Component scores are generated from the elements of $\mathbf{A}_{ap}$ according to the following expression:

$$g_{\mathrm{ap}}(i,n) = \sum_{p=1+(i-1)J}^{iJ} a_{\mathrm{ap}}(p,n) \quad (2)$$

in which $g_{ap}(i,n)$ is the score for the component n in the ith sample, extracted from the nth chromatographic subprofile of $\mathbf{A}_{ap}$.

The three-way Augmented PARAFAC model of Equation 1 should be unique and would not require constraints for successful decomposition [8]. However, as discussed below for the studied water samples, some constraints were necessary for adequate resolution. Therefore, the new strategy includes the option to restrict the system with similar constraints to those regularly employed in the case of MCR-ALS (i.e., non-negativity and unimodality), which can be imposed on individual profiles along each mode and in each subarray of the augmented data set. Also, the correspondence among species and samples in the case of samples containing uncalibrated interferents can be applied. Figure 1 shows the flow chart of the Augmented PARAFAC model. For a better understanding, it is recommended to see Figure 1S in the Electronic Supplementary Material, which corresponds to the flow chart of the MCR-ALS model, and compare it with Figure 1.

Details on MCR-ALS are provided in the Electronic Supplementary Material for comparison.

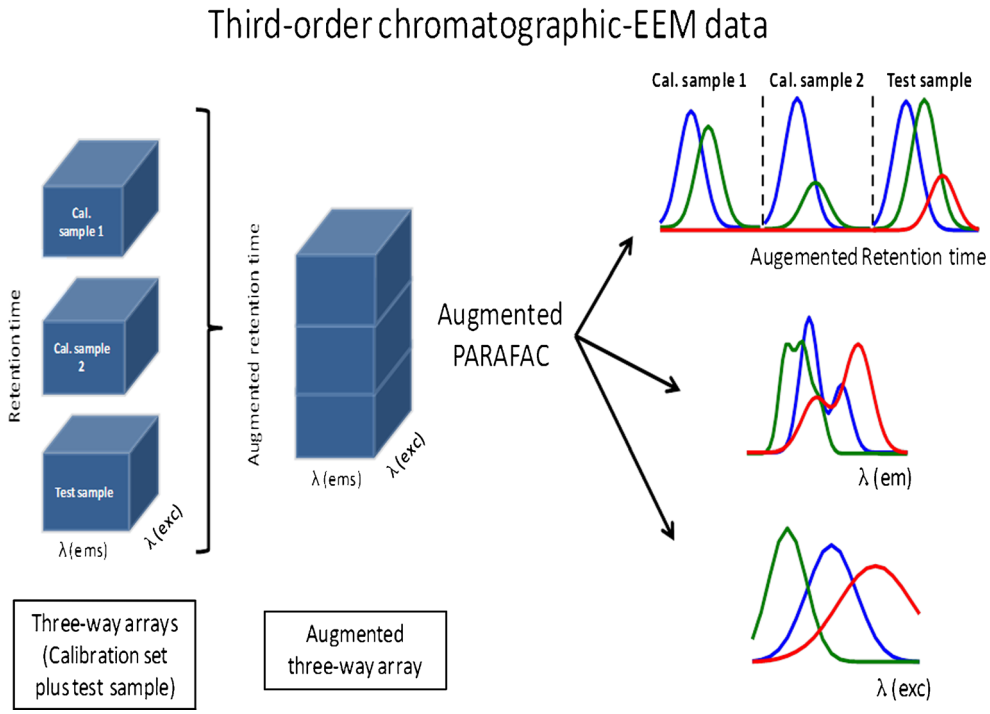

Fig. 1 Flow chart of Augmented PARAFAC to third-order chromatographic-EEM data processing

Experimental

Chemicals and reagents

All standards were of analytical grade. Ofloxacin (OFL) and enoxacin (ENO) were provided by Sigma, Seelze, Germany. Ciprofloxacin (CPF) and danofloxacin (DNF) were purchased from Fluka, Buchs, Switzerland. Marbofloxacin (MRF) was provided by Molekula, Shaftesbury, UK. Methanol and acetonitrile, both of LC grade, were obtained from J.T. Baker, Deventer, The Netherlands. Ultrapure water was obtained with a Milli-Q water purification system from Millipore, Bedford, USA. Acetic acid was purchased from Cicarelli (San Lorenzo, Argentina) and sodium acetate trihydrate was provided by Anedra (Tigre, Argentina).

Calibration, validation and real samples

Stock standard solutions of the five pharmaceuticals were prepared in methanol, all at a concentration of 350 mg L^{-1}, and were maintained at 4 °C in the dark. Working standard solutions were prepared daily by dilution of the stock standard solutions in water. Tap, commercial mineral, and well water were used to prepare the test samples.

A calibration set of 12 standard samples was prepared by transferring appropriate aliquots of OFL, CPF, and DNF stock solutions to 25.0 mL volumetric flacks and completing to the mark with ultrapure water. The calibration set was built following a fractional central composite design (α=1.41) with one center replicate. The final concentrations were between 0.0 and 100.0 μg L^{-1} for OFL, between 0.0 and 150.0 μg L^{-1} for CPF, and between 0.0 and 25.0 μg L^{-1} for DNF.

A 10-sample validation set was built considering concentrations of OFL, CPF, and DNF different than those used for calibration. Additionally, MRF and ENO were incorporated at different concentrations as uncalibrated interferences in the 10 validation samples. The validation set was prepared by transferring appropriate aliquots of the stock solution of each FQ to 25.0 mL volumetric flacks and completing to the mark with ultrapure water.

Six real samples were spiked at three different concentration levels for each FQ. MRF and ENO were also incorporated as uncalibrated interferences. Real samples were prepared by transferring appropriate aliquots of the stock solution of each FQ to 25.0 mL flasks and completing to the mark with tap, commercial mineral, or well water.

Finally, all solutions were subjected to pre-concentration data collection and processing in the same way. Final concentrations in validation and real samples are summarized in Tables 1 and 2.

Solid-phase extraction (SPE) procedure

The SPE experiments were performed using commercial Oasis HLB cartridges (Milford, USA) preconditioned with 1.0 mL of methanol and 2.0 mL of ultrapure water. Samples (25.0 mL) were introduced into the preconditioned cartridges at a flow rate of approximately 3 mL min^{-1}. After that, the cartridges were washed with 2.0 mL of ultrapure water. Since the elution was performed with 250.0 μL methanol, a 100-fold

Table 1 Results obtained for validation samples[a]

Sample	Ofloxacin			Ciprofloxacin			Danofloxacin		
	Nom.	Pred.		Nom.	Pred.		Nom.	Pred.	
		MCR-ALS	AP		MCR-ALS	AP		MCR-ALS	AP
1	20.0	21.1	20.1	90.0	99.3	92.5	25.0	27.1	23.2
2	20.0	19.3	19.7	150.0	131.0	121.7	15.0	16.4	15.9
3	60.0	51.1	52.1	30.0	44.9	58.5	5.0	5.3	5.1
4	100.0	101.0	99.7	90.0	95.8	90.9	5.0	8.6	8.9
5	60.0	68.1	70.1	150.0	144.8	147.0	25.0	28.4	28.8
6	100.0	98.9	99.1	150.0	132.7	136.9	15.0	17.8	18.2
7	100.0	104.1	101.0	30.0	21.0	22.0	5.0	7.4	7.6
8	20.0	31.0	31.7	30.0	58.0	51.7	2.0	4.0	4.0
9	60.0	45.3	55.2	30.0	19.8	25.6	8.0	9.6	9.4
10	60.0	55.1	72.3	60.0	54.2	44.3	2.0	5.3	2.6
RMSEP		7	7		14	16		2	2
REP (%)		14.5	13.8		19.0	21.5		19.9	19.1

[a] Nom. = nominal, Pred. = predicted, AP=Augmented PARAFAC, all concentrations in μg L^{-1}, REP (%), relative error of prediction, RMSEP, root mean square error of prediction in μg L^{-1}

pre-concentration factor was achieved. The extract was injected directly into the chromatographic system.

HPLC-EEM procedure

The chromatographic studies were performed on an Agilent 1100 LC instrument (Agilent Technologies, Waldbronn, Germany), equipped with degasser, quaternary pump, autosampler, oven column compartment, UV-visible diode array detector, fluorescence detector, and the ChemStation software package to control the instrument, data acquisition, and data analysis. The analytical column used was a Zorbax Eclipse XDB-C18, 75 mm×4.6 mm, 3.5 μm particle size (Agilent Technology).

The column temperature was controlled by setting the oven temperature at 35 °C. The mobile phase consisted in a 10 mmol L^{-1} acetic acid buffer (pH=4.0) acetonitrile-methanol mixture (71:9:20, v/v). Samples were analyzed in

Table 2 Results obtained for real samples[a]

Sample	Ofloxacin			Ciprofloxacin			Danofloxacin		
	Added	Pred.		Added	Pred.		Added	Pred.	
		MCR-ALS	AP		MCR-ALS	AP		MCR-ALS	AP
Tap									
	20.0	30.6	17.4	30.0	26.3	25.0	3.5	3.2	2.9
	60.0	81.2	63.8	90.0	78.6	91.2	5.5	7.5	7.6
Ground									
	60.0	61.9	65.3	90.0	86.6	89.5	2.2	2.7	2.6
	40.0	32.2	26.2	60.0	60.5	62.9	9.0	12.8	12.4
Mineral									
	20.0	12.5	19.1	30.0	19.7	17.0	2.2	1.9	1.9
	40.0	41.1	49.9	60.0	91.1	81.3	9.0	9.5	9.2
Rec (%)		106	98		98	97		116	113
RMSEP		11	7		14	10		2	2
REP (%)		21.3	15.0		19.1	14.0		14.4	13.1

[a] Nom. = nominal, Pred. = predicted, AP=Augmented PARAFAC, all concentrations in μg L^{-1}, REP (%), relative error of prediction, RMSEP, root mean square error of prediction in μg L^{-1}, Rec (%): average recovery

isocratic mode. The complete analysis was carried out in 3 min. The flow rate was maintained at 1.80 mL min^{-1}. Samples were filtered through 0.22 μm nylon membrane filters before injection.

At the end of the chromatographic procedure, each fraction was collected every 2 s in a 96-wells plate, which is usually employed for enzyme-linked immunosorbent assays (ELISA). The collection started after 37 s from the initial time of the chromatographic run, and it continued during 50 s, in such a way that 25 fractions were collected for each run. The ELISA plate was set at the end of the LC instrument and operated with a homemade device, which automatically moves the plate, allowing the collection of 60 μL in every well. This volume was optimized according to the smaller volume that can be read by the fluorimeter.

All spectrofluorimetric measurements were performed using a Perkin-Elmer LS-55 luminescence spectrometer (Waltham, USA) equipped with a plate reader accessory coupled to an optical fiber and a gated photomultiplier connected to a PC microcomputer via a RS232C connection. Excitation-emission fluorescence matrices were collected varying the emission wavelength between 380 and 500 nm each 2.5 nm, and registering the excitation spectra from 260 to 340 nm each 2.5 nm. Hence, the size of each data matrix was 17×25. The slit widths for both excitation and emission monochromators were fixed at 10 nm, and the detector voltage at 600 V.

Software

The ChemStation software (Agilent Technologies) was employed for LC instrument control. Two graphical user interfaces (GUI) were written in Processing 2.0b6 [22] for serial communication between the computer and Arduino UNO (operating the sampler) [23], and to the fluorimeter. Visual controls were made from the Processing control P5 controller library form, which can be incorporated into the processing integrated development environment (IDE) after installation. The first GUI was made for controlling the Arduino board by sending parameters for automatic sampling (delay, number of wells, time between wells) or to manually controlling the position in real time. The second GUI was installed in the PC for communication with the fluorimeter, and was responsible for sending parameters to the fluorimeter (wavelengths, slits, scan speed, number of wells) and for sequentially plotting spectra once they were collected. The model Arduino UNO board was programmed with the IDE 1.0.1 language.

All employed models were implemented in MATLAB 7.6 [24]. Those for applying MCR-ALS are available in the Internet at http://www.mcrals.info/. Augmented PARAFAC was developed as an in-house code inspired in those provided by Bro in his webpage http://www.models.life.ku.dk/nwaytoolbox/download.

Results and discussion

Third-order data generation

Figure 2A shows a chromatogram for validation sample No. 1 (Table 1) containing OFL, CPF, DNF, MRF, and ENO (these two latter compounds were added as unexpected components), registered at λ_{exc}=291 nm and λ_{em}=495 nm. As can be seen, the five substances cannot be completely separated by the chromatographic method, but the procedure only requires 84 s to be carried out, attaining the highly recommended green analytical chemistry principles [4]. On the other hand, Figure 2B shows excitation and emission spectra of OFL (λ_{exc}=291 nm, λ_{em}=495 nm), CIP (λ_{exc}=273 nm, λ_{em}=448 nm), DNF (λ_{exc}=278 nm, λ_{em}=441 nm), MRF (λ_{exc}=295 nm, λ_{em}=505 nm), and ENO (λ_{exc}=265 nm, λ_{em}=424 nm), allowing us to conclude about the high complexity of the system under study. Interestingly, the selectivity can be improved taking advantage of the differences in the excitation and emission spectra. Thus, 25 fractions were collected every 2 s for each chromatographic run, and then complete EEMs were registered for each collected fraction. Figure 3 shows the contour plots of six EEMs corresponding to different fractions collected between 41 and 62 s for validation sample No. 1. A visual inspection of this figure makes it apparent the large amount of information that can be obtained by collecting the data using the above commented procedure.

It should be stressed that the simultaneous quantitation of OFL, CPF, and DNF in the presence of two uncalibrated compounds, which highly interfere in the analysis (see Figures 2 and 3), has been performed for the first time by using the present approach. Hypothetically, this methodology has the potentiality of being adapted to a high number of complex chromatographic applications and, in this way, it may contribute with a two-fold improvement to new chromatographic-chemometric techniques: (1) it can be implemented to solve a fairly tough problem in the field of chemometrics (i.e., the misalignment of analyte chromatographic peaks in different runs [25] because under this new paradigm the changes in peak shapes are naturally incorporated as a feature for each analyte, and (2) as the number of third-order applications increases, new analytical advantages may be uncovered and added to the already known second-order advantage of third-order data [26].

On the other hand, by obtaining an EEM at every chromatographic time, more information will be available compared with the recording of the emission spectrum at a single excitation wavelength (or vice versa), selected as a compromise between the optimal wavelengths for each analyte. Consequently, maximum information for every target analyte can be gathered exciting at all possible wavelengths, with the interesting advantage, independently of the chemometric modeling, that excitation and emission wavelengths are

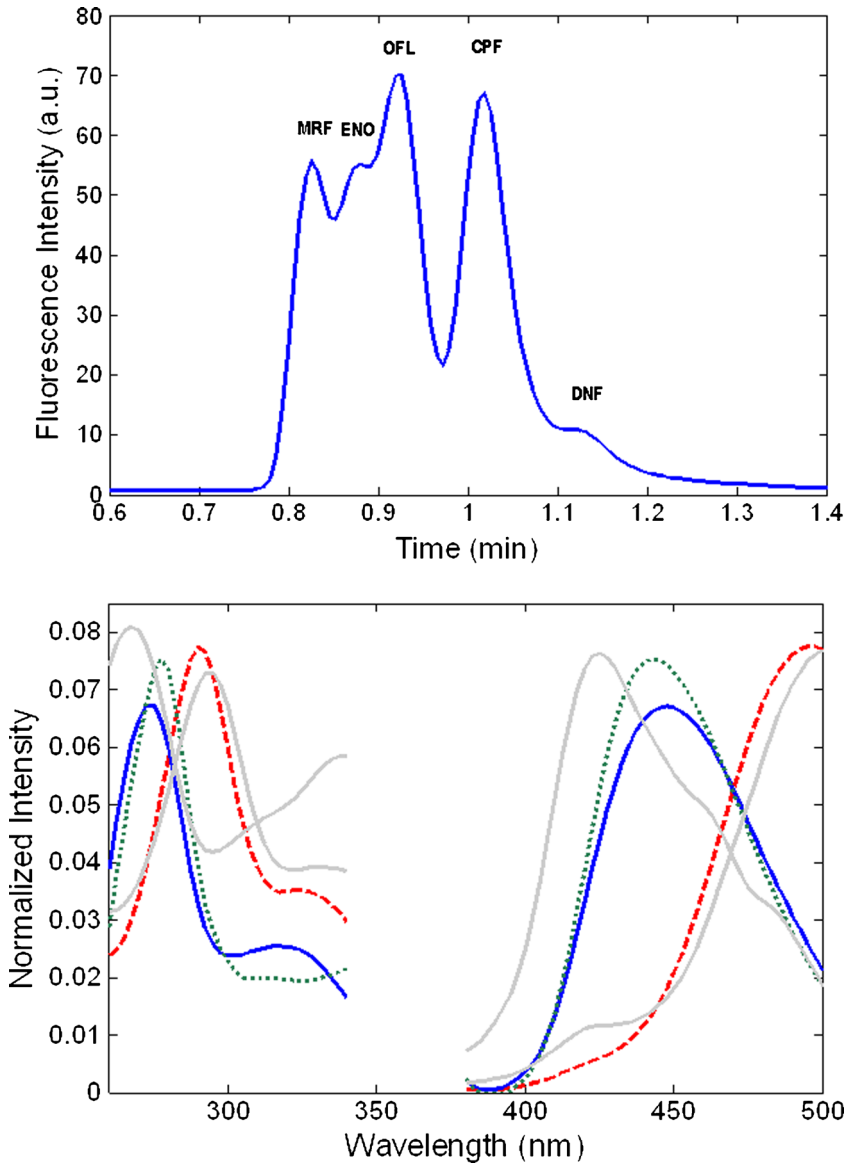

Fig. 2 (**A**) Chromatogram for validation sample No. 1 (Table 1) containing the three quantitated FQs and the two unexpected components, registered at λ_{exc}=291 nm and λ_{em}=495 nm. (**B**) Excitation and emission spectra of CPF, blue solid line; OFL, red dashed line; DNF, green dotted line; MRF and ENO, grey lines. Each of these spectra was obtained at the optimum excitation and emission wavelengths for each compound

optimized, and useful information for peak identification can be retrieved.

Finally, it is worth mentioning that the methodology employed here is not the only form to collect third-order chromatographic EEM data. Until now, two additional strategies were proposed: (1) several chromatographic runs were performed for each sample, recording emission spectra of each one at different excitation wavelengths, which were selected according to the excitation spectra of the compounds of interest [6], and (2) a single chromatographic run was performed for each sample, recording EEMs in several fractions [7]. In the present work, the latter experimental procedure was adopted because it is experimentally simpler than the former one, and avoids lack of reproducibility between successive injections for the same individual sample.

MCR-ALS modeling

With the purpose of quantitating OFL, CPF, and DNF in validation and test samples, super-augmented data matrices were built for each unknown sample by suitably appending the calibration data matrices ($\mathbf{D}_{mcr}$; see Electronic Supplementary Material). The following constraints were applied during the ALS optimization to get physically meaningful solutions: (1) correspondence between common species in the different data matrices, (2) concentration and spectral profiles were constrained to be non-negative, and (3) unimodality was imposed in all concentration sub-profiles. The number of components was estimated by singular value decomposition, and it was used to build the initial estimations, the spectra of which were obtained by selection of the so-called purest variables [27]. After MCR-ALS decomposition of $\mathbf{D}_{mcr}$

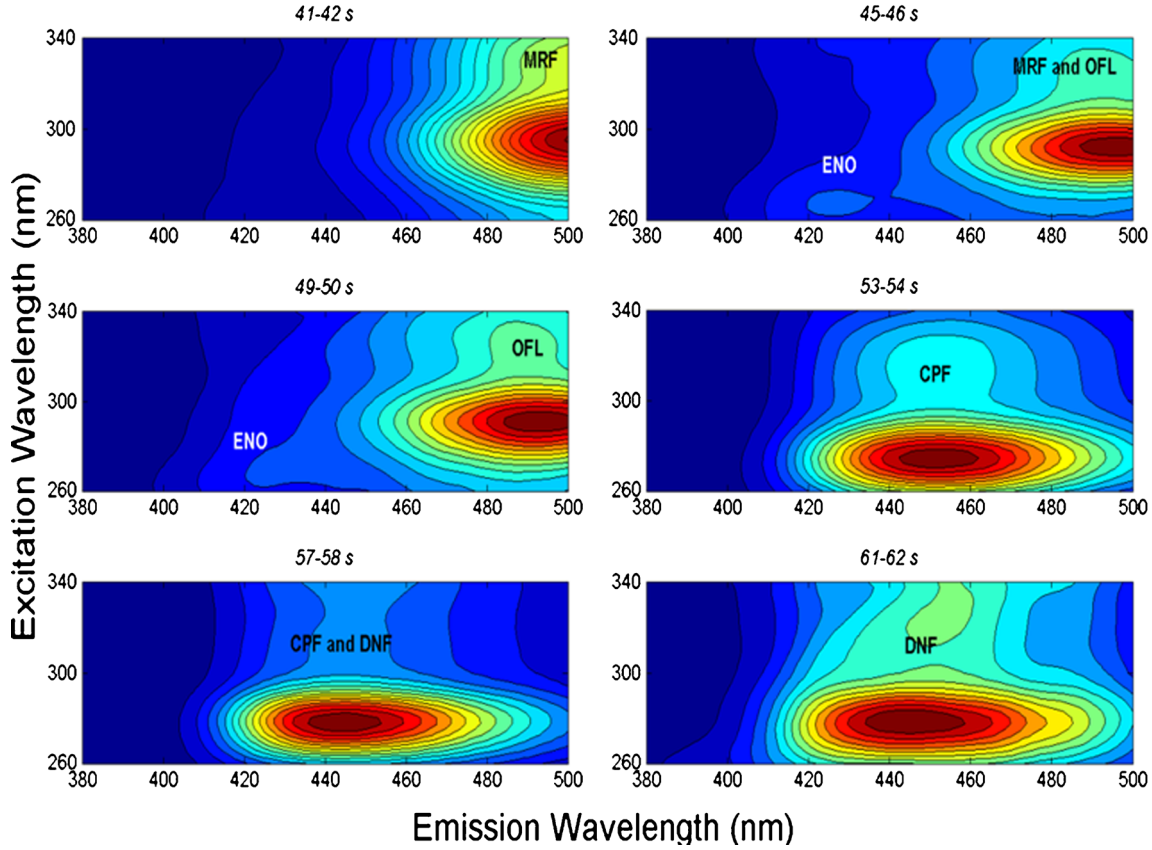

Fig. 3 Contour plots of six EEMs corresponding to different fractions: 41-42 s, 45-46 s, 49-50 s, 53-54 s, 57-58 s, and 61-62 s, collected for the validation sample No. 1. The presence of analyte peaks are indicated

according to Equation 1S, the concentration information contained in $\mathbf{C}_{mcr}$ was used to construct the pseudo-univariate graph by plotting the analyte concentration scores against the nominal analyte concentrations (see Equation 2S). The analyte predictions are displayed in Tables 1 and 2.

Figure 4 shows the profiles retrieved by MCR-ALS for validation sample No. 1. The model outputs are presented in Figure 4A and B (time and unfolded EEM profiles, respectively). Figure 4C shows the emission and excitation profiles of all compounds present in the sample, obtained via refolding of the profile matrix in the non-augmented mode ($\mathbf{S}_{mcr}^{T}$; see Electronic Supplementary Material). This refolding was made for each component by first reshaping the corresponding row of ($\mathbf{S}_{mcr}^{T}$) into a matrix, submitting the latter to singular value decomposition, and taking the first left and right eigenvectors as estimations of the true component profiles in both data modes. This process is essential to reliably determine that the obtained information is in good agreement with the experimental data. This is in contrast to Augmented PARAFAC, which directly retrieves excitation and emission spectral profiles for each component. More importantly, the sensitivity of the MCR-ALS may be lower than that of Augmented PARAFAC because the data are unfolded, as mentioned above. Nevertheless, in the present case, the refolded spectral profiles for the analytes and the interferents were very similar to the experimental ones, which are shown in Figure 2B. This is consistent with the obtained analytical performance, as can be appreciated in Table 1.

Regarding the time profiles, it is important to note that each component profile (analytes or interferents) is composed of concatenated chromatograms (the calibration set and the test sample), i.e., each time profile is a vector of size 325×1, (325=25×13, corresponding to 25 time sensors, 12 calibration samples, and 1 test sample, i.e., 13 samples). It is worth recalling that the matrix $\mathbf{C}_{mcr}$ is of size 325×5 (three analytes and two interferents). The individual columns of $\mathbf{C}_{mcr}$ are submitted to Equation 2S to predict the concentration of the analytes of interest in the sample test. It is important to notice that significant shifts are present in the analyte chromatographic profiles from run to run. In fact, for the analyzed sample shown in Figure 2, there are differences between 4 and 9 s in peak maxima for OFL, CPF, and DNF among the 13 chromatographic runs. The shift ranges are shown on the top of Figure 4A as time bars, and represent more than 10 % of the total chromatographic time. The retrieved profiles are in good agreement with the experimental data (not shown).

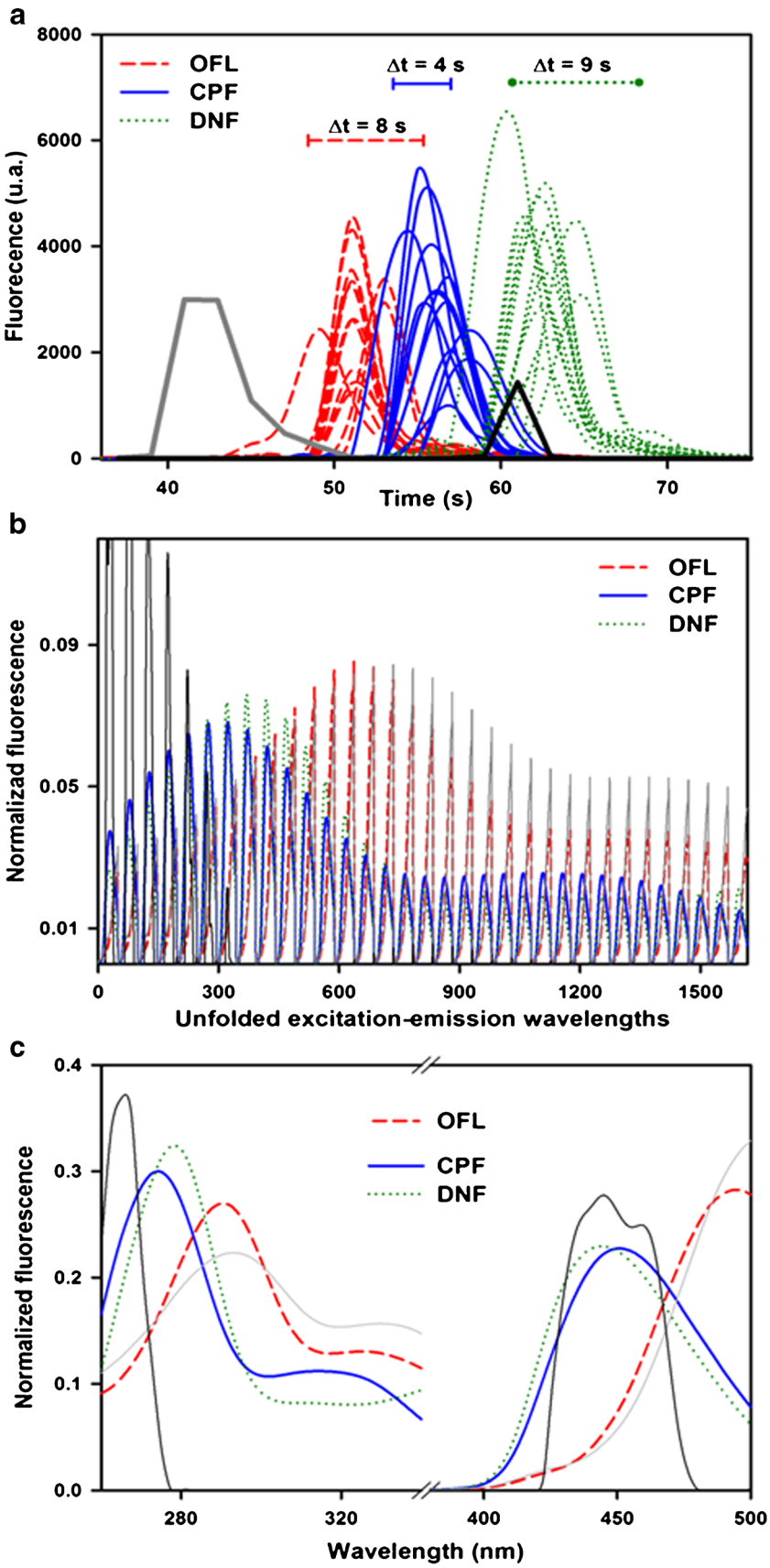

Fig. 4 Profiles retrieved by MCR-ALS analysis of third-order data for validation sample No. 1 (Table 1), containing the three quantitated FQs and two unexpected components. (**A**) Temporal profiles, with time bars indicating the maximum shifts for each analyte; (**B**) unfolded EEM profiles; (**C**) refolding of unfolded EEM profiles to obtain the excitation and emission profiles (see text). CPF, blue solid line; OFL, red dashed line; DNF, green dotted line; profiles for MRF and ENO in grey lines

Augmented PARAFAC modeling

In principle, the application of this model only involves an initialization step because no constraints are necessary due to the fact that the decomposition of a trilinear three-way array is often unique [8]. However, preliminary results based on unrestricted decompositions were inadequate. In any case, further research is required on additional third-order experimental data in order to conclude on the need of applying restrictions during the least-squares fit to the Augmented PARAFAC model.

In order to improve the versatility of the new strategy, the same kind of constraints regularly applied in MCR-ALS were implemented, i.e., unimodality, non-negativity, and correspondence among analytes and samples (for more details, see above). In the case of the validation samples, during optimization the following constraints were appropriate: (1) concentration and spectral profiles were constrained to be non-negative, (2) concentration sub-profiles were restricted to be unimodal, and (3) correspondence between components and samples was included, informing the algorithm that interferents were absent from the calibration samples.

Augmented PARAFAC was then used to determine the concentrations of OFL, CPF, and DNF simultaneously in the test samples, which contain MRF and ENO as potential interferents. At first, an augmented three-way array was built

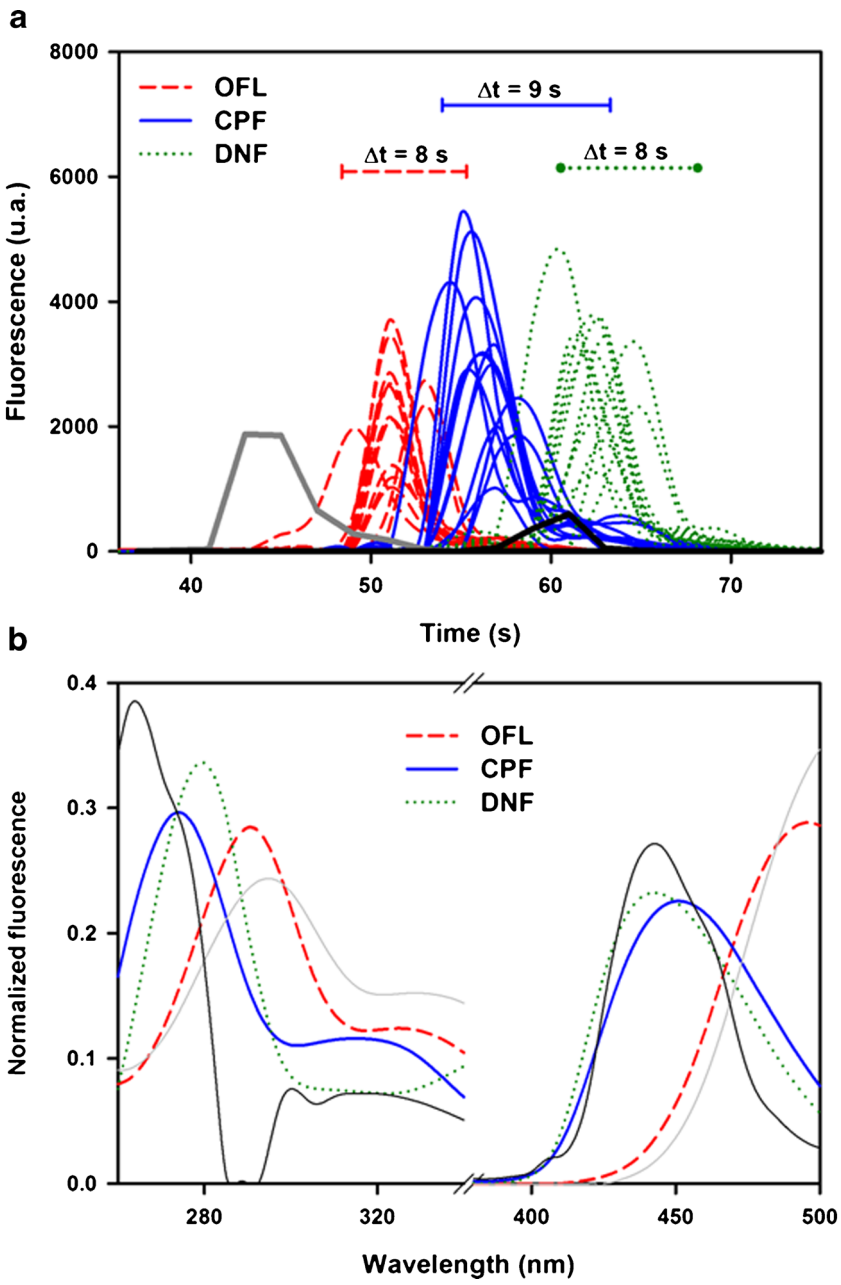

Fig. 5 Profiles retrieved by Augmented PARAFAC for validation sample No. 1 (Table 1), containing the three quantitated FQs and two unexpected components. (**A**) Temporal profiles; (**B**) excitation and emission profiles, obtained by fixing the sensor values at λ_{exc}= 295 nm and λ_{em}=452 nm (for more details, see text). CPF, blue solid line; OFL, red dashed line; DNF, green dotted line; both for profiles and time bars, MRF and ENO, grey lines

by appending an unknown sample plus the 12 calibration arrays. Upon optimization, both the number of five pure components (three analytes and two interferents) and their spectra were estimated according to the Theory section. Finally, and analogously to MCR-ALS model, the concentration information contained in $\mathbf{A}_{ap}$ was used to construct the univariate graph by plotting the analyte concentration scores (Equation 2) against the nominal analyte concentrations. The predictions obtained are displayed in Tables 1 and 2.

Figure 5 shows the profiles resolved by Augmented PARAFAC for the validation sample No. 1. In contrast to MCR-ALS, the output includes the individual excitation and emission spectral profiles (Figure 5B) as well as time profiles (Figure 5A). As shown for MCR-ALS modeling, the spectral profiles are in good agreement with the experimental data (Figure 2B).

With regard to the matrix $\mathbf{A}_{ap}$ (which includes the unfolded profiles along the combined sample-elution time modes and contains concentration information regarding the responsive constituents), its meaning and information content is analogous to $\mathbf{C}_{mcr}$ in the context of MCR-ALS. Hence, Augmented PARAFAC is also able to identify substantial shifts in elution time shapes of the analyte profiles, as Figure 5A shows (see the time bars on top of the time profiles, implying differences of up to 9 s in the 13 runs for OFL, CPF, and DNF). Interestingly, these results are very consistent with both MCR-ALS and experimental data.

Comparison of quantitative results

In order to compare the performance of the two models in terms of predictive ability and figures of merit when modeling the present third-order data, predictions obtained on the 10 validation samples and the six real samples presented in Tables 1 and 2 were statistically compared using the randomization test proposed by Van der Voet to compare prediction errors [28]. The result indicates that the root mean square errors of prediction (RMSEPs) found by MCR-ALS are not significantly different than those obtained by Augmented PARAFAC, since the probability values obtained for the three analytes is considerably smaller than the critical level of 0.05.

Regarding the set of validation samples, Figure 6 shows the MCR-ALS and Augmented PARAFAC predicted concentrations of OFL, CPF, and DNF as a function of the nominal values. In each sample analyzed, the potential interferents MRF and ENO were added at random concentrations. In line with the statistical analysis mentioned above, the performance of the new strategy is matched satisfactorily with MCR-ALS. Indeed, as can be seen in Table 1, acceptable relative errors of prediction (REP, in %) are achieved in all cases. Interestingly, it is not only as satisfactory as those obtained by MCR-ALS but also as good as the results reported in similar, less complex cases [7].

Table 3 shows the computed figures of merit for the models employed when analyzing the validation set samples. While expressions for MCR-ALS figures of merit are known [29], appropriate expressions for Augmented PARAFAC have not been developed [30]. In this work, we have used an extension of the previously derived expressions [30], although they may be overoptimistic. It should be emphasized that the enhancement in sensitivity (SEN) and excellent values of limits of detection (LODs) and limits of quantification (LOQs) were found for both models for OFL, CPF, and DNF, and similar to those for third-order analysis of water samples of lower complexity [7]. Also, better figures of merit were found for Augmented PARAFAC in comparison with MCR-ALS for all the analytes.

We finally discuss the results concerning the real samples. Because drinking waters did not contain the studied FQs, they were spiked with the analytes and also with the potential interferents, and a recovery study was carried out. Three different water samples (tap, mineral, and underground) were

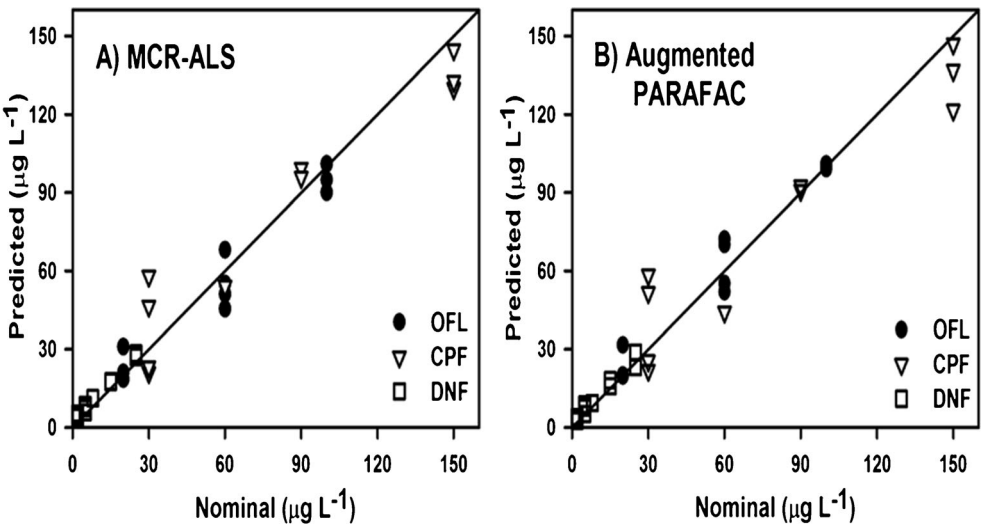

Fig. 6 Plots of predicted concentrations of the studied analytes as a function of the nominal values in test samples with interferences. (**A**) MCR-ALS; (**B**) Augmented PARAFAC. OFL, black circles; CPF, white triangles; DNF, white squares

Table 3 Figures of merit for the validation samples[a]

Figure of merit	Ofloxacin		Ciprofloxacin		Danofloxacin	
	MCR-ALS	AP	MCR-ALS	AP	MCR-ALS	AP
SEN	10.4	21	2.7	20	22.9	83
SEL	0.68	0.65	0.21	0.29	0.22	0.30
[Anal. SEN]$^{-1}$	0.08	0.01	0.30	0.01	0.04	0.01
LOD (μg L^{-1})	0.25	0.20	0.99	0.15	0.12	0.02
LOQ (μg L^{-1})	0.75	0.60	2.97	0.47	0.36	0.08

[a] AP, Augmented PARAFAC, SEN, sensitivity, calculated according to Ref [29] for MCR-ALS, and to Ref [30] for AP, SEL, selectivity, calculated according to Ref [29] for MCR-ALS, and to Ref [30] for AP, Anal. SEN, analytical sensitivity, calculated as sensitivity/s_{test} (s_{test}, noise level), LOD, limit of detection, calculated according to Ref [29] for MCR-ALS, and to Ref [30] for AP, LOQ: limit of quantitation, calculated according to LOD × (10/3.3)

tested, each containing two different analyte levels, which were in the concentration ranges indicated in the Experimental section. The complexity of these samples is very similar to the validation samples and, thus, the profiles resolved by both models are essentially the same as those shown in Figure 4 (MCR-ALS) and Figure 5 (Augmented PARAFAC). The results in terms of the elliptical joint confidence region (EJCR) accuracy test are shown in Figure 7. The elliptical domains obtained for all samples, analytes and models contain the theoretically predicted values for the slope (1) and intercept (0), and therefore the methods can be considered accurate. Interestingly, some improvement in precision is detected for Augmented PARAFAC, since the size of its EJCR is smaller than for MCR-ALS.

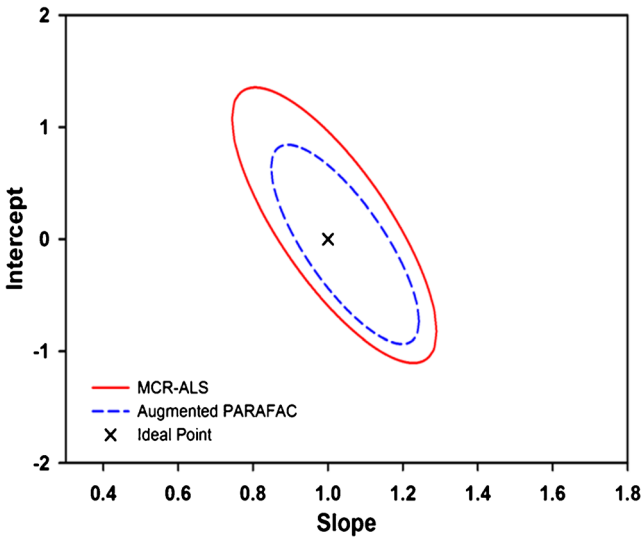

Fig. 7 Elliptic joint confidence region (EJCR) tests for the prediction results of OFL, CPF, and DNF in test samples for MCR-ALS (red solid line); Augmented PARAFAC (blue dashed line)

Finally, it should be noted that PARAFAC2 was also applied, but the results were not satisfactory owing to the poor predictions obtained with this algorithm. As was commented above, PARAFAC2 is more flexible regarding changes in elution profiles from sample to sample, but it is less useful in the presence of interferents, as is the case of the system under study in this work [15].

Augmented PARAFAC is an adequate option for processing chromatographic third-order data, furnishing acceptable results in samples containing various calibrated analytes and interferents. Moreover, the performance of the new strategy is as good as that for MCR-ALS for third-order chromatographic data.

Conclusions

Third-order data obtained through excitation–emission matrices at different elution times were employed to simultaneously determine three fluoroquinolones in tap, underground, and mineral waters spiked with uncalibrated components. To process these data, a new PARAFAC model inspired in the augmentation concept of MCR-ALS was implemented. Augmented PARAFAC achieves the second-order advantage even in the presence of sample-to-sample changes in temporal profiles, similarly to MCR-ALS. The analytical method saves cost and time, and is in accordance with the green analytical chemistry principles, preserving acceptable analytical qualities. Indeed, the relative error predictions (in %) found for OFL, CPF, and DNF in drinking water samples (15.0 %, 14.0 %, and 13.1 %, respectively) are even better than those found by MCR-ALS (21.3 %, 19.1 %, and 14.4 %, respectively). The two applied strategies for processing third-order chromatographic-EEM data were rigorously compared. The proposed Augmented PARAFAC approach shows a number of advantages. One of them is the possibility of processing the measured data in the original three-dimensional structure, instead of unfolding the data to arrays of lower dimensions. This eventually leads to improved analytical predictions and better figures of merit, as demonstrated through a suitable experimental example.

Acknowledgments The authors are grateful to Universidad Nacional del Litoral (Projects CAI+D 2012 No. 11-11), Universidad Nacional de Rosario, CONICET (Consejo Nacional de Investigaciones Científicas y Técnicas, Project PIP 455), and ANPCyT (Agencia Nacional de Promoción Científica y Tecnológica, Projects PICT 2011-0005 and PICT 2013-0136) for financial support. M.R.A. thanks CONICET for her fellowship.

References

1. Escandar GM, Goicoechea HC, Muñoz de la Peña A, Olivieri AC (2014) Second- and higher-order data generation and calibration: a tutorial. Anal Chim Acta 806:8–26

2. Escandar GM, Faber NM, Goicoechea HC, Muñoz de la Peña A, Olivieri AC, Poppi RJ (2007) Second and third-order multivariate calibration: data, algorithms, and applications. Trends Anal Chem 26:752–765
3. Booksh KS, Kowalski BR (1994) Theory of analytical chemistry. Anal Chem 66:782A–791A
4. Gałuszka A, Migaszewski Z, Namiesnik J (2013) The 12 principles of green analytical chemistry and the SIGNIFICANCE mnemonic of green analytical practices. Trends Anal Chem 50:78–84
5. Parastar H, Radovic JR, Jalali-Heravi M, Diez S, Bayona JM, Rn T (2011) Resolution and quantification of complex mixtures of polycyclic aromatic hydrocarbons in heavy fuel oil sample by means of GC×GC-TOFMS combined to multivariate curve resolution. Anal Chem 83:9289–9297
6. Lozano VA, Muñoz de la Peña A, Durán-Merás I, Espinosa Mansilla A, Escandar GM (2013) Four-way multivariate calibration using ultra-fast high-performance liquid chromatography with fluorescence excitation–emission detection. Application to the direct analysis of chlorophylls *a* and *b* and pheophytins a and b in olive oils. Chemom Intell Lab Syst 125:121–131
7. Alcaráz MR, Siano GG, Culzoni MJ, Muñoz de la Peña A, Goicoechea HC (2014) Modeling four and three-way fast high-performance liquid chromatography with fluorescence detection data for quantitation of fluoroquinolones in water samples. Anal Chim Acta 809:37–46
8. Olivieri AC, Escandar GM (2014) Practical three-way calibration. Elsevier, Waltham
9. Bortolato SA, Lozano VA, Muñoz de la Peña A, Olivieri AC (2014) Novel augmented parallel factor model for four-way calibration of high-performance liquid chromatography-fluorescence excitation-emission data. Chemom Intell Lab Syst. doi:10.1016/j.chemolab.2014.11.013
10. Bro R (1998) Multi-way analysis in the food industry. Models, algorithms, and applications. Doctoral Thesis, University of Amsterdam, The Netherlands
11. Xia AL, Wu HL, Li SF, Zhu SH, Hu LQ, Yu RQ (2007) Alternating penalty quadrilinear decomposition algorithm for an analysis of four-way data arrays. J Chemometr 21:133–144
12. Fu H, Wu H, Yu Y, Yu Y, Zhang S, Nie J, Li S, Yu RQ (2011) A new third-order calibration method with application for analysis of four-way data arrays. J Chemometr 25:408–429
13. Tauler R (1995) Multivariate curve resolution applied to second order data. Chemom Intell Lab Syst 30:133–146
14. Bloemberg TG, Gerretzen J, Lunshof A, Wehrens R, Buydens LMC (2013) Warping methods for spectroscopic and chromatographic signal alignment: a tutorial. Anal Chim Acta 781:14–32
15. Bortolato SA, Olivieri AC (2014) Ultra performance liquid chromatography tandem mass spectrometry performance evaluation for analysis of antibiotics in natural waters. Anal Chim Acta 842:11–19
16. Tamtam F, Mercier F, Eurin J, Chevreuil M, Le Bot B (2009) Ultra performance liquid chromatography tandem mass spectrometry performance evaluation for analysis of antibiotics in natural waters. Anal Bioanal Chem 393:1709–1718
17. Speltini A, Sturini M, Maraschi F, Profumo A (2010) Fluoroquinolone antibiotics in environmental waters: sample preparation and determination. J Sep Sci 33:1115–1131
18. Parrilla Vázquez MM, Parrilla Vázquez P, Martínez Galera M, Gil García MD (2012) Determination of eight fluoroquinolones in groundwater samples with ultrasound-assisted ionic liquid dispersive liquid–liquid microextraction prior to high-performance liquid chromatography and fluorescence detection. Anal Chim Acta 748:20–27
19. Cañada-Cañada F, Arancibia JA, Escandar GM, Ibañez GA, Espinosa Mansilla A, Muñoz de la Peña A, Olivieri AC (2009) Second-order multivariate calibration procedures applied to high-performance liquid chromatography coupled to fast-scanning fluorescence detection for the determination of fluoroquinolones. J Chromatogr A 1216:4868–4876
20. Alcaráz MR, Vera-Candioti L, Culzoni MJ, Goicoechea HC (2014) Ultrafast quantitation of six quinolones in water samples by second order capillary electrophoresis data modeling with multivariate curve resolution-alternating least squares. Anal Bioanal Chem 406:2571–2580
21. Bro R (1997) PARAFAC. Tutorial and applications. Chemom Intell Lab Syst 38:149–171
22. Processing Free and Open Source Software. Available at: http://processing.org/. Accessed 10 Jan 2015
23. Arduino Free and Open Source Software. Available at: http://arduino.cc. Accessed 10 Jan 2015
24. MATLAB 7.6 (2008) TheMathWorks Inc., Natick, MA, USA
25. Olivieri AC, Escandar GM, Muñoz de la Peña A (2011) Second-order and higher-order multivariate calibration methods applied to non-multilinear data using different algorithms. Trends Anal Chem 30:607–617
26. Olivieri AC (2008) Analytical advantages of multivariate data processing. One, two, three, infinity? Anal Chem 80:5713–5720
27. Windig W, Guilment J (1991) Interactive self-modeling mixture analysis. Anal Chem 63:1425–1432
28. van der Voet H (1994) Comparing the predictive accuracy of models using a simple randomization test. Chemom Intell Lab Syst 25:313–323
29. Bauza C, Ibañez GA, Tauler R, Olivieri AC (2012) Sensitivity equation for quantitative analysis with multivariate curve resolution-alternating least-squares: theoretical and experimental approach. Anal Chem 84:8697–8706
30. Olivieri AC, Faber K (2012) New developments for the sensitivity estimation in four-way calibration with the quadrilinear parallel factor model. Anal Chem 84:186–193